since this composition represents the iodinated phase with smallest value of x (ref 2 and see below), and similarly for the $TTFI_x$ phase of lowest iodine content.

We are also interested in the energetics of the formation of more highly iodinated $TTFI_x$ phases, according to the generalized reaction

$$D + (x_i/2)I_2 \rightarrow DI_{x_i} \quad (A4)$$

where $i > 1$. If a cathode is prepared from a mixture of two adjacent line phases DI_{x_j} and DI_{x_k}, $x_k > x_j$, then the cell with silver anode will give a voltage $\delta E°(k,j)$ corresponding to

$$(x_k - x_j)Ag + DI_{x_k} \rightarrow (x_k - x_j)AgI + DI_{x_j} \quad (A5)$$

$$E = \delta E°(k,j)$$

and the free energy for the reaction

$$((x_k - x_j)/2)I_2 + DI_{x_j} \rightarrow DI_{x_k} \quad (A6)$$

$$E = E_{AgI}° - \delta E°(k,j)$$

is simply the difference in formation free energies of DI_{x_j} and DI_{x_k}:

$$\Delta G(DI_{x_k}) - \Delta G(DI_{x_j}) = (x_j - x_k)F(E_{AgI}° - \delta E°(k,j)) \quad (A7)$$

Thus, the free energy of formation for any phase of interest can be calculated if the free energies are known for the reaction of eq A2 and for all transformations between adjacent line phases with lower I content, according to eq A6.

The $TTFI_x$ phase with $x = 2.0$–2.3 is not fully treated in the above analysis because it is not a true line phase and because of the observation of two structural modifications within this phase.[5] Then, to be rigorous, we should treat each point within the phase range independently. Also, the composition-independent voltage of cells with this as the lower iodine phase means that the last entry in Table II should have $x_j = 2.3$. However, the composition range for this quasi-line phase is very narrow, the two reported structures are quite similar, and most important, our experiments indicate that there is a negligible free energy change across the composition range: cells prepared from independent batches of "$TTFI_2$" having slightly different stoichiometries showed no discernible differences. Therefore, we treat this phase as a single composition, taking $x = 2$. This treatment is supported by the binding energy calculations done by Torrance and Silverman[1b] for $TTFBr_x$, $x = 0.71$–0.76. They found less than 0.25% change in the binding energy over the observed phase range. Both $TTFBr_x$, $x = 0.71$–0.76, and $TTFI_x$, $x = 2.0$–2.3 (or $x = 0.70$–0.72), have segregated stacks and about the same ionicity so that, qualitatively at least, we would expect the binding energy to behave similarly in both materials.

Registry No. $H_2(Pc)I$, 33606-65-4; $TTFI_{0.71}$, 77547-33-2; $TTFI_2$, 64265-34-5; $TTFI_3$, 55492-88-1; $(CH_3)_4NI_3$, 4337-68-2.

Crystal Structure of Tetrapropylammonium Fluoride Containing Precursor to Fluoride Silicalite

Geoffrey D. Price,[†1] Joseph J. Pluth,[†] Joseph V. Smith,*[†] J. Michael Bennett,[‡] and R. Lyle Patton[‡]

Contribution from the Department of the Geophysical Sciences, The University of Chicago, Chicago, Illinois 60637, and the Union Carbide Corporation, Tarrytown, New York 10591.
Received January 8, 1982

Abstract: A precursor to fluoride silicalite was crystallized from a hydrothermal system containing silica, tetrapropylammonium ion (TPA^+), and fluoride (F^-). Single-crystal X-ray diffraction data for a twinned crystal (180 × 50 × 50 μm) of the precursor were refined in space group *Pnma* ($a = 20.044$ (2), $b = 19.918$ (4), and $c = 13.395$ (2) Å). The a axis of one twin component is parallel with the b axis of the other. Combined X-ray intensities (hkl and khl) were separated in a least-squares refinement. The silica framework has the same topology as that of silicalite and ZSM-5 zeolite. A weak negative correlation between the secant of angle (Si–O–Si) and Si–O is consistent with molecular-orbital models. The TPAF has similar geometry to tetrapropylammonium bromide and lies at the intersection of the 10-ring channels of the framework in a position consistent with a template mechanism of crystallization. The end carbon atoms of propyl groups lie 2.7 and 3.1 Å away from the end carbon atoms of adjacent propyl groups, and there is insufficient room for replacement of propyl by *n*-butyl. Oblique optical extinction and slight anomalies in high-angle X-ray diffractions indicate monoclinic symmetry, but the sharpness of X-ray powder diffractions limits angular deviations to less than 0.1° from orthogonal geometry. Slight collapse of the framework and positional disorder of the TPAF may be responsible.

Fluoride silicalite is a new microporous silica polymorph,[2] similar in some properties to silicalite,[3] and the hydrophobic and organophilic nature of these materials may prove commercially important for the removal of organic compounds from wastewater. The framework linkage of silicalite[3] is topologically the same as that of synthetic high-silica zeolite ZSM-5,[4,5] a shape-selective catalyst[5–8] capable of converting methanol into water and hydrocarbons, useful in internal-combustion engines.

The precursor of fluoride silicalite[2] crystallizes from a hydrothermal system containing silica, tetrapropylammonium (TPA^+), and fluoride (F^-) ions, and the ideal chemical composition is $TPAF{\cdot}Si_{24}O_{48}$. Because of the suggestion[3,9–11] that quaternary ammonium cations can act as templates around which tetrahedral frameworks assemble during crystallization, the crystal structure

† The University of Chicago.
‡ Union Carbide.

(1) Present address: Department of Earth Sciences, Cambridge University, Cambridge, England CB2 3EQ.
(2) Flanigen, E. M.; Patton, R. L. U.S. Patent NM4 073 865, 1978.
(3) Flanigen, E. M.; Bennett, J. M.; Grose, R. W.; Cohen, J. P.; Patton, R. L.; Kirchner, R. L.; Smith, J. V. *Nature (London)* **1978**, *271*, 512–516.
(4) Argauer, R. J.; Landolt, G. R. U.S. Patent NM3 702 886, 1972.
(5) Kokotailo, G. T.; Lawton, S. L.; Olson, D. H.; Meier, W. M. *Nature (London)* **1978**, *272*, 437–438.
(6) Kokotailo, G. T.; Meier, W. M. *Spec. Publ.-Chem. Soc.* **1980**, *33*, 133–139.
(7) Meisel, S. L.; McCullough, J. P.; Lechthaler, C. H.; Weisz, P. B. *CHEMTECH* **1976**, *6*, 86–89.
(8) Naccache, C.; Benn Taarit, Y. In "Proceedings of the Fifth International Conference on Zeolites"; Rees, L. V. C., Ed.; Heyden: London, 1980.

0002-7863/82/1504-5971$01.25/0

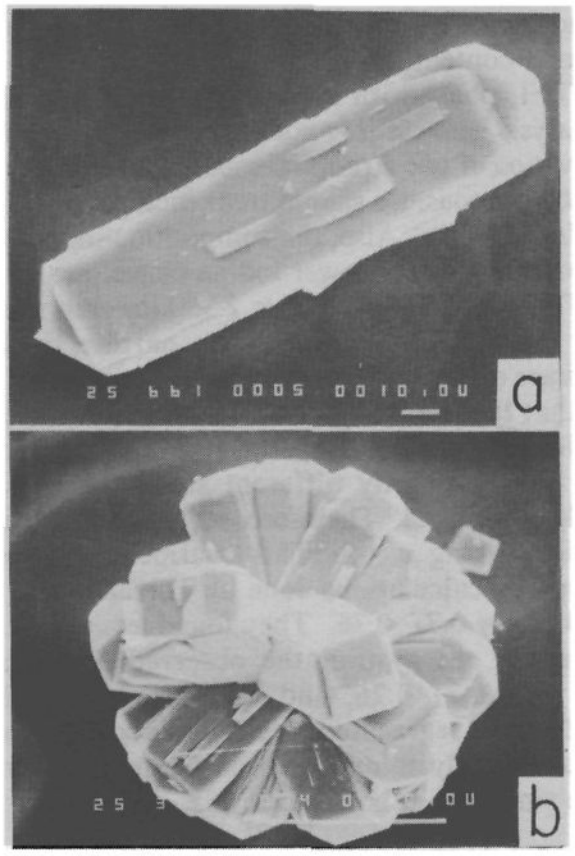

Figure 1. Scanning electron micrographs of TPAF-precursor crystals to fluoride silicalite: (a) twinned crystal showing wedge-shaped crystallites on all {100} faces, scale bar 10 μm; (b) rosette of crystals, scale bar 100 μm. Diffraction intensities from the wedge-shaped crystallites were too small to affect seriously the data collection.

of the precursor was determined.[12] Reference will be made to the crystal structure of silicalite[3] obtained by calcination of a precursor synthesized in a non-fluoride system. The atomic coordinates thereof are of low accuracy because of (a) the difficulty of collecting and refining X-ray data from the small crystals and (b) the problems caused by interpenetrant twinning and monoclinic, pseudoorthorhombic symmetry.[13] Revised atomic coordinates for this silicalite were presented[14] for a refinement based on the pseudo space group *Pnma*.

After completion of the present structure determination of the precursor to fluoride silicalite,[12] the detailed crystal structure and structure-related properties of an as-synthesized ZSM-5 was published by Olson et al.[15] The ZSM-5 crystal is apparently untwinned, orthorhombic with space group *Pnma*, cell dimensions $a = 20.07$ (1), $b = 19.92$ (1), and $c = 13.42$ (1) Å. Its chemical composition is $M_xAl_{1.1}Si_{94.9}O_{192}$, where M is a mixture of Na and tetraalkyl cations of unspecified nature whose positions were not located except for two positions labeled Ox1 and Ox2. Although the framework topologies of the fluoride silicalite precursor and ZSM-5 are the same, there are some differences in the cell dimensions and atomic coordinates of the frameworks as should be expected considering the different chemical compositions of the framework and nonframework constituents. Particularly important in the present study of the precursor to fluoride silicalite is the location of the TPAF complex within the channels of the silica framework.

Optical and X-ray Study

The crystals of the fluoride silicalite precursor used in this study occur as either interpenetrant twins (Figure 1a) or polycrystalline rosettes (Figure 1b). The larger of the two twin components (Figure 2) has pyramidal boundaries with the two pieces of the second component, and if untwinned, both components would be tablets elongated along *c* of size

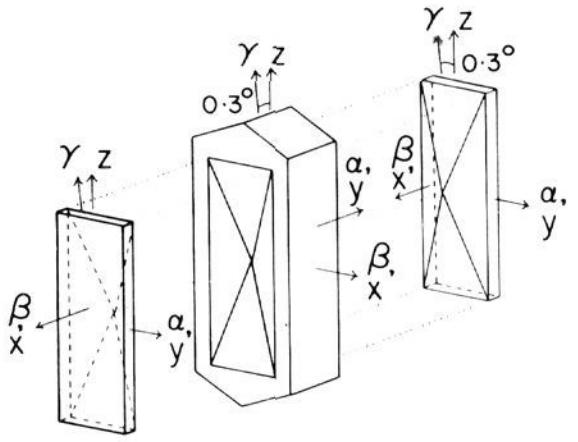

Figure 2. Exploded representation of interpenetrant twinning of a crystal as in Figure 1a. The central, major twin component is structurally related to the two parallel minor components by a 90° rotation about [001]. Directions of the crystallographic axes *a*, *b*, and *c* and the principal axes of the optical indicatrix α, β, and γ are shown. The measured values of the principal refractive indices for Na D light are α 1.491, β 1.493, and γ 1.496. The observed correspondence of the optical β and crystallographic *a* axes is consistent with the report[13] that the *a* axis is the crystallographic symmetry axis for a silicalite in space group $P2_111$ and that the crystallographic angle α is not orthogonal.[16]

~180 × 50 × 50 μm. Electron microprobe analyses showed only SiO_2 and no Al_2O_3 at the detection level (<0.02 wt %).

Because of the pseudotetragonal geometry of the fluoride silicalite precursor, the twin morphology was interpreted with the aid of X-ray diffraction methods. Weissenberg photographs about the *c* axis of the precursor showed pairs of diffractions, and high-angle spots showed that a_1 and b_2 are strictly parallel, as are a_2 and b_1, where the suffixes refer to the two twin components. Slight angular deviation for the {110} diffractions rules out reflection twinning on {(110)}, and the geometrical relations fit 90° rotation about the *c* axis, even though part of the twin boundaries are approximately {(110)}. Comparison of diffraction intensities allowed identification with the morphological twin units and indexing of the major crystallographic forms as {(101)} and {(100)}; most of the {(010)} form is replaced by the other twin component.

Although the diffraction geometry appears to be orthogonal with $a = 20.044$ (2), $b = 19.918$ (4), and $c = 13.395$ (2) Å, measured by four-circle diffraction goniometry, the optical symmetry appears to be very slightly monoclinic, with an extinction angle of 0.3°. The optical orientation is shown in Figure 2, and the difference in double refraction of the twin components results in an hourglass pattern under crossed polars. To check the orthogonality of the unit cell, we examined a powder diffractometer pattern for splitting or broadening of appropriate diffractions. A specimen of silicalite was shown to be monoclinic by X-ray single-crystal methods,[13] and a powder diffraction pattern of a different specimen of silicalite[16] with splitting of the 131 and 352 diffractions could be indexed with a cell geometry of $a = 20.117$ (5), $b = 19.874$ (5), and $c = 13.371$ (4) Å; $\alpha = 90.62$ (1)°. No broadening of these or any other lines was found for the fluoride silicalite precursor, and the interaxial angles must be 90° within 0.1°.

Because of the difficulty of resolving the nearly superimposed *hkl* and *khl* diffractions of the fluoride silicalite precursor, the combined intensity of each pair was collected for a hemisphere out to $\sin\theta/\lambda = 0.42$. The data were measured and a fixed θ–2θ scan at 0.75°/min with monochromatized Mo Kα radiation (λ 0.7093 Å) and a Picker diffractometer automated by KRISEL. The scan width in °2θ was $2.0 + 0.7 \tan\theta$, and the total counting time for background was 120 s per diffraction. Because the resulting 7237 diffractions obeyed orthorhombic symmetry, only a further octant of data was recorded for $0.42 < \sin\theta/\lambda < 0.65$. Averaging the 12088 diffractions yielded 6829 unique ones of which 1645 were above background at the 2σ level. Seven diffraction intensities were later found to fit poorly with calculated intensities and were omitted after a recheck showed an error in the original measurement. Absences would fit with both *Pnma* and $Pn2_1a$, and structure refinement proceeded satisfactorily in the centric space group. Accurate cell dimensions were obtained by least-squares refinement of 2θ values for eight intense diffractions ($75.8 < 2\theta < 81.2$) by using Cu $K\alpha_1$ radiation.

The estimated errors in the intensities (α_1) were calculated by $\alpha_1 \approx P[S + t^2B + (k(S + tB))^2]^{1/2}$, where *P* is the scan rate, *S* is the peak scan count, *B* is the total background count, *t* is the ratio of peak-to-total-background observation time, and *k* is an instability constant (0.02).

(9) Flanigen, E. M. *Adv. Chem. Ser.* **1973**, *No. 121*, 119–139.
(10) Aiello, R.; Barrer, R. M. *J. Chem. Soc. A* **1970**, 1470–1475.
(11) Grose, R. W.; Flanigen, E. M. U.S. Patent NM4 061 724, 1977.
(12) Price, G. D.; Pluth, J. J.; Smith, J. V.; Araki, T.; Bennett, J. M. *Nature (London)* **1981**, *292*, 818–819.
(13) Bennett, J. M.; Cohen, J. P.; Kirchner, R. M. *Am. Crystallogr. Assoc. Meet. Abstr.* **1979**, *6*, 62.
(14) Smith, J. V. In "Fifth International Conference on Zeolites—Recent Progress Reports and Discussions"; Sersale, R., Colella, C., Aiello, R., Eds.; Heyden: London, 1981; pp 218–225.
(15) Olson, D. H.; Kokotailo, G. T.; Lawton, S. L.; Meier, W. M. *J. Phys. Chem.* **1981**, *85*, 2238–2243.
(16) Taramasso, M.; Perego, G.; Notari, B. In "Proceedings of the Fifth International Conference on Zeolites"; Rees, L. V. C., Ed.; Heyden: London, 1980.

Symmetry-equivalent diffractions were averaged by using $\bar{I} = \sum_i(I_i/\sigma_i^2)/\sum_i\sigma_i^{-2}$ and $\sigma(\bar{I}) = [N/(N-1)\sum_i\sigma_i^{-2}]^{1/2}$, where I_i and σ_i are the intensity and the standard deviation of the ith equivalent reflection. The intensity data were corrected for Lorentz and polarization effects assuming a monochromator crystal half-perfect and half-mosaic. No absorption correction was applied, because the transmission factor varied with orientation only between 96.6% and 95.2%.

Structure Refinement

The refinement of the structure of the precursor was achieved with the program TWXLLS, which is a structure-factor least-squares program developed[17,18] specially to deal with the intensity data obtained from twinned crystals and which allows the relative volumes of the two twin components to be included as one of the variables in the least-squares cycles. This can be achieved if the calculated structure amplitude ($F_c(hkl)$), which is compared to the observed structure amplitude ($F_o(hkl)$), is expressed in terms of the volume fraction of the two twin components. If the volume fraction (V) of the two twin components (1 and 2) is given by $V_1 + V_2 = 1$ and if the twinning is such that $(hkl)_1$ and $(khl)_2$ are related, the total $F_c^2(hkl)$ can be expressed as

$$F_c^2(hkl) = V_1F_c^2(hkl)_1 + V_2F_c^2(khl)_2$$

assuming that the diffractions from each twin component are mutually incoherent. The resulting derivatives are

$$\delta F/\delta V_1 = (F_{c_1}^2 - F_{c_2}^2)/2F_c$$

and

$$\delta F/\delta X = (T_1V_1 + T_2V_2)/F_c$$

where X is a spatial parameter and T_i is given by

$$T_i = A_i\frac{\delta A_i}{\delta X} + B_i\frac{\delta B_i}{\delta X}$$

A and B are the real and imaginary components of the structure factor, respectively.

No difficulty was experienced in obtaining a refinement of the TPAF silicalite precursor framework with this program and in using as starting parameters those determined[14] for the framework of silicalite. The cycles of least squares minimized $\sum w||F_o| - |F_c||^2$ with $w = \sigma_F^{-2}$. Atomic scattering factors and anomalous scattering corrections for Si^{2+} and O^- were taken from Volume IV of "International Tables for X-ray Crystallography". The factors for Si^{2+} were obtained from interpolation between factors for Si and Si^{4+}. The refinement, however, could not proceed beyond a state with $R = 0.10$, and at this point a difference Fourier map was calculated to show the positions of the nonframework atoms. This map was constructed by comparing the effective structure amplitude of the first twin component ($F_c(hkl)_1V_1^{1/2}$) with a scaled F_o. The F_o was scaled to take into account only the contribution of twin component 1 by the function

$$F_{scaled}(hkl) = F_o(hkl)F_c(hkl)_1V_1^{1/2}/F_c(hkl)$$

Sections of the difference Fourier map (Figure 3) showed the position of the organic molecule at the intersection of the 10-ring channels. The position of the F^- ion was less well-defined, however, and it was placed in an approximately toroidal region of electron density (Figure 4), also located close to the 10-ring intersection. On the inclusion of one TPAF complex per channel intersection, with F^- fixed on the mirror plane at $y = 0.75$ close to the centroid of the toroidal region, the weighted R dropped to 0.0715 after four cycles of least-squares refinement. Isotropic displacement parameters were used for the framework atoms, and a group displacement parameter was used for the TPAF complex. At this stage, a discrepancy remained between the calculated and observed electron density for F^-, and further cycles of least-squares refinement were performed in which the occupancy of the F^- site was halved and it was allowed to refine to a position off the mirror plane. After four cycles, for which individual displacement parameters were used for the atoms of the TPAF complex, the weighted residuals dropped to 0.0665. The resulting configuration of the TPAF complex was not physically sensible, however, with some F–C distances ranging between 1.1 and 1.6 Å. It is felt that the toroidal electron density represents both positional disorder of the F^- ion and the lower true symmetry of the structure and that the refinement of the complex in which the F^- ion is fixed on the mirror plane at $y = 0.75$ gives a more representative, or time-averaged, view. Accordingly, the coordinates, bond lengths, and bond angles in Tables I and II are those for the refinement in which the F^- ion was placed at the

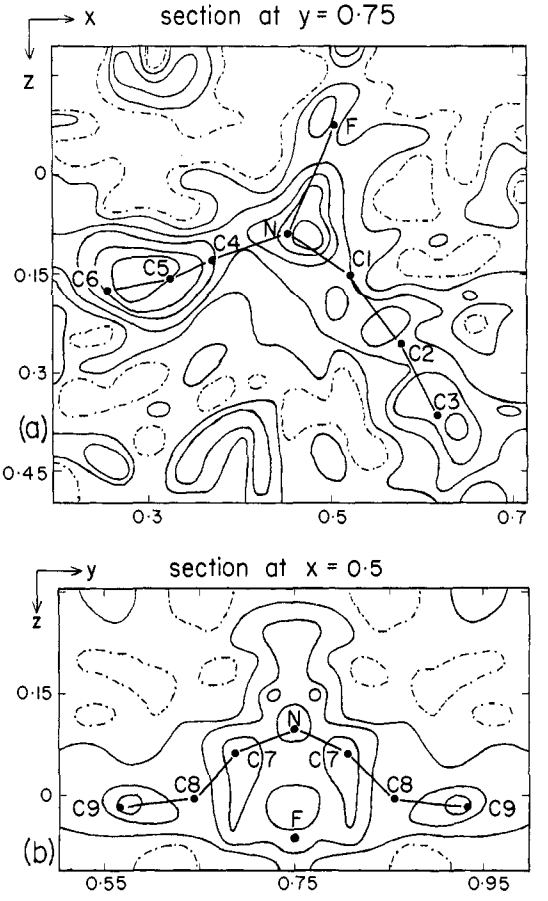

Figure 3. Difference Fourier maps of electron density associated with nonframework atoms in the precursor: (a) section in mirror plane at $y = 0.75$; (b) section normal to the mirror plane. The projections of the refined positions of the atoms in the TPAF complex are projected onto the sections. Contours spaced at 0.20 e Å^{-3}. Zero contour is dot-dashed.

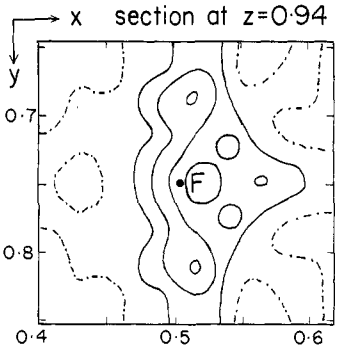

Figure 4. Electron density associated with the F atom shown in a section normal to the mirror plane at $y = 0.75$. The toroid is interpreted to result from positional disorder, and the least-squares refinement of the position of the F atom lies at the centroid of the electron density. Contours spaced at 0.20 e Å^{-3}.

centroid of the toroid of electron density.

The final residual electron density on a difference Fourier map was generally low (less than ±0.25 e Å^{-3}) except in the region of the TPAF complex and those framework oxygens in special positions on the mirror planes at $y = 0.25$ and 0.75. For the nonframework atoms, the electron density residuals range between −0.4 and +0.5 e Å^{-3}, and some kind of spatial disorder is responsible. Residual electron density up to 0.7 e Å^{-3} for the oxygen atoms (O1, O5, O22, O26) is attributed to movement away from the assumed mirror plane of *Pnma* into a general position of a space group that lacks the mirror plane. No attempts were made to make refinements in space groups of lower symmetry because of the very strong correlations[14] that would occur in the least-squares matrix.

The refined value of the relative twin volumes (42:58) corresponds well with an estimate from optical microscopy. To index the faces, we resolved high-angle diffractions using Cu Kα radiation for a twin in known

(17) Araki, T. *Am. Crystallogr. Assoc. Meet. Abstr.* **1977**, *5(2)*, 68.
(18) Araki, T. *Am. Crystallogr. Assoc. Meet. Abstr.* **1977**, *7(1)*, 36.

Table 1. Atomic Coordinates in *Pnma*

TPAF precursor to fluoride silicalite					ZSM-5[15]				
atom[a]	x	y	z	B	x	y	z	B	atom[b]
Si1	0.1215 (5)	0.3256 (5)	0.9731 (8)	2.2 (2)	0.1199 (6)	0.3271 (6)	0.9731 (10)	1.8 (3)	T10
Si2	0.2741 (5)	0.3252 (5)	0.9715 (8)*	2.5 (2)	0.2748 (6)	0.3278 (6)	0.9634 (10)*	1.6 (3)	T9
Si3	0.0767 (4)	0.4412 (6)	0.8365 (7)*	1.7 (2)	0.0768 (5)	0.4395 (7)	0.8306 (9)*	1.0 (3)	T1
Si4	0.0712 (4)	0.3690 (5)	0.1825 (7)	2.1 (2)	0.0702 (6)	0.3696 (6)	0.1826 (10)	1.0 (3)	T11
Si5	0.3144 (4)	0.4403 (5)	0.8318 (7)*	2.1 (2)	0.3116 (8)	0.4427 (7)	0.8249 (9)*	2.0 (3)	T6
Si6	0.3079 (5)	0.3710 (4)	0.1878 (6)	1.9 (2)	0.3076 (9)	0.3714 (7)	0.1848 (11)	2.2 (3)	T8
Si7	0.0732 (4)	0.5271 (4)	0.1867 (7)	1.7 (2)	0.0728 (7)	0.5278 (6)	0.1822 (13)	1.9 (3)	T5
Si8	0.3081 (6)	0.5296 (4)	0.1925 (6)*	2.2 (2)	0.3090 (9)	0.5281 (5)	0.1849 (11)*	1.9 (3)	T2
Si9	0.3128 (5)	0.6736 (4)	0.8215 (7)	1.8 (2)	0.3106 (8)	0.6742 (5)	0.8172 (9)	1.2 (2)	T12
Si10	0.2798 (3)	0.5601 (5)	0.9710 (6)	2.0 (2)	0.2788 (5)	0.5602 (8)	0.9688 (10)	2.1 (3)	T3
Si11	0.1225 (4)	0.5634 (5)	0.9718 (6)	2.0 (2)	0.1220 (6)	0.5641 (7)	0.9674 (9)	1.4 (3)	T4
Si12	0.0763 (5)	0.6710 (5)	0.8278 (9)	2.3 (2)	0.0768 (7)	0.6695 (7)	0.8258 (13)	2.7 (3)	T7
O1	0.1139 (17)	1/4	0.9279 (24)	4.6 (9)	0.1089 (23)	1/4	0.9420 (34)	2.7 (11)	O26
O2	0.1956 (11)	0.3466 (7)	0.9631 (12)	3.3 (4)	0.1981 (17)	0.3459 (10)	0.9676 (17)	3.7 (5)	O9
O3	0.0819 (10)*	0.3705 (13)	0.8874 (17)	2.9 (5)	0.0909 (13)*	0.3742 (15)	0.8870 (21)	2.9 (6)	O15
O4	0.0943 (13)	0.3370 (13)	0.0841 (23)	6.0 (8)	0.0909 (16)	0.3348 (18)	0.0751 (25)	4.4 (9)	O10
O5	0.2911 (12)	1/4	0.9456 (15)	1.0 (5)	0.2861 (14)	1/4	0.9410 (23)	0.5 (7)	O25
O6	0.3154 (8)	0.3705 (10)	0.8910 (12)	1.9 (4)	0.3153 (11)	0.3705 (12)	0.8824 (16)	1.3 (5)	O18
O7	0.3099 (13)	0.3493 (8)	0.0729 (14)	3.0 (4)	0.3079 (18)	0.3486 (11)	0.0681 (17)	3.0 (6)	O8
O8	0.9957 (8)	0.5430 (12)	0.2125 (15)	2.4 (5)	0.9984 (12)	0.5425 (13)	0.2056 (19)	1.9 (6)	O21
O9	0.3705 (10)	0.5533 (18)*	0.2457 (14)	3.5 (5)	0.3728 (14)	0.5665 (15)*	0.2397 (19)	2.8 (6)	O1
O10	0.0875 (11)	0.5011 (10)	0.9170 (15)	2.9 (5)	0.0840 (15)	0.5011 (18)	0.9177 (24)	4.0 (8)	O16
O11	0.0814 (8)	0.4511 (13)	0.1763 (14)	3.9 (4)	0.0790 (12)	0.4474 (22)	0.1743 (20)	4.4 (6)	O14
O12	0.1153 (11)*	0.3400 (11)*	0.2667 (16)	3.0 (5)	0.1230 (18)*	0.3573 (22)*	0.2632 (26)	6.1 (9)	O11
O13	0.9976 (9)	0.3478 (9)	0.2046 (14)	1.7 (4)	0.9984 (14)	0.3435 (13)	0.2078 (20)	1.9 (6)	O22
O14	0.3858 (9)	0.4420 (13)	0.7807 (12)	1.7 (4)	0.3817 (10)	0.4408 (15)	0.7697 (13)	0.8 (4)	O5
O15	0.2566 (8)	0.4363 (13)*	0.7463 (12)	2.5 (4)	0.2593 (14)	0.4560 (16)*	0.7418 (21)	3.6 (7)	O6
O16	0.2946 (11)	0.4982 (9)	0.9096 (13)	3.2 (5)	0.2963 (16)	0.4970 (15)	0.9020 (22)	3.2 (7)	O19
O17	0.3083 (11)	0.4481 (11)	0.1921 (13)	5.8 (5)	0.3112 (17)	0.4481 (21)	0.1823 (20)	5.6 (7)	O13
O18	0.2542 (11)*	0.6506 (13)*	0.7489 (19)	4.5 (6)	0.2529 (14)	0.6660 (14)*	0.7393 (21)	2.9 (7)	O12
O19	0.3753 (12)	0.3390 (12)*	0.2389 (17)	3.1 (6)	0.3750 (15)	0.3491 (16)*	0.2361 (21)	3.0 (7)	O7
O20	0.0986 (9)	0.5606 (12)	0.0857 (14)	3.3 (5)	0.1000 (15)	0.5571 (26)	0.0817 (23)	4.9 (8)	O4
O21	0.3072 (9)	0.5618 (8)	0.0836 (11)*	1.9 (3)	0.3095 (13)	0.5621 (12)	0.0761 (13)*	1.7 (5)	O2
O22	0.3038 (16)	3/4	0.8485 (16)	2.3 (5)	0.2955 (17)	3/4	0.8476 (23)	1.4 (7)	O24
O23	0.3125 (11)	0.6302 (9)	0.9196 (12)	2.9 (4)	0.3090 (20)	0.6259 (17)	0.9147 (22)	4.9 (8)	O20
O24	0.2033 (10)	0.5612 (10)	0.9702 (12)	4.4 (4)	0.1993 (18)	0.5605 (16)	0.9737 (18)	5.4 (6)	O3
O25	0.0988 (10)	0.6319 (11)	0.9280 (16)	2.4 (5)	0.1024 (15)	0.6300 (16)	0.9191 (22)	3.1 (7)	O17
O26	0.0729 (13)	3/4	0.8603 (21)	2.9 (7)	0.0723 (19)	3/4	0.8503 (28)	2.4 (9)	O23
N	0.4501 (42)	3/4	0.1053 (57)	19.4 (1.3)					
C1	0.5373 (49)	3/4	0.1532 (80)	19.4 (1.3)					
C2	0.5810 (66)	3/4	0.2670 (84)	19.4 (1.3)					
C3	0.6121 (52)	3/4	0.3735 (77)	19.4 (1.3)					
C4	0.3631 (56)	3/4	0.1519 (77)	19.4 (1.3)	0.3770 (68)	3/4	0.1210 (94)	0.7	Ox2
C5	0.3259 (64)	3/4	0.1724 (113)	19.4 (1.3)	0.3254 (33)	3/4	0.1485 (50)	0.7	Ox1
C6	0.2610 (45)	3/4	0.1866 (114)	19.4 (1.3)					
C7	0.4835 (36)	0.6867 (38)	0.0642 (58)	19.4 (1.3)					
C8	0.5044 (35)	0.6456 (32)	0.9964 (57)	19.4 (1.3)					
C9	0.5032 (24)	0.5675 (32)	0.9852 (54)	19.4 (1.3)					
F	0.5072 (27)	3/4	0.9433 (49)	19.4 (1.3)					

[a] Standard deviation (1σ) in parentheses. Nomenclature from ref 14. [b] Nomenclature from ref 15. Asterisk refers to coordinates that differ by more than 3 times the sum of the standard deviations.

optical orientation, and intensity measurements were compared with values estimated from the twin volumes and the calculated structure amplitudes.

Discussion

The silica framework of the TPAF-containing precursor to fluoride silicalite has the same topology as both the silica framework of silicalite[3,19] and the aluminosilicate framework of ZSM-5.[5,6,15] The 96 tetrahedral sites per unit cell plus the 192 oxygen atoms generate a four-connected tetrahedral framework containing a system of intersecting channels bounded by 10-rings, as shown in stereoplots.[5,15] A simplified drawing of the channel system (Figure 5) shows how straight channels parallel to *b* connect with zig-zag channels along [101] and [10$\bar{1}$] to give four-pointing intersections. Figure 6 shows how a TPAF complex lies at each intersection, with a propyl limb lying along each of the four channels and a fluorine atom tucked in between carbon atoms from three propyl limbs. The C3 and C6 end atoms of two propyl limbs pointing along zig and zag components of a zig-zag channel approach too closely to allow addition of another C atom

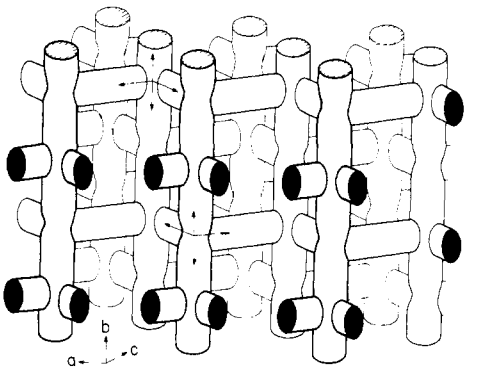

Figure 5. Idealized drawing of channel system in a silicalite type of framework. Each straight channel along *b* is shown as a cylinder. Segments of cylinders along [101] and [10$\bar{1}$] fit together to form each zig-zag channel along *a*.

(19) Smith, J. V. In "Proceedings of the Fifth International Conference of Zeolites"; Rees, L. V. C., Ed.; Heyden: London, 1980; pp 194–204.

Table II. Interatomic Distances (Å) and Angles (Deg) in TPAF Precursor to Fluoride Silicalite[a]

Si1-O1	1.629 (16)	Si5-O6	1.599 (21)	Si9-O12	1.640 (25)
O2	1.548 (24)	O14	1.587 (19)	O18	1.593 (26)
O3	1.658 (25)	O15	1.631 (18)	O22	1.575 (10)
O4	1.600 (32)	O16	1.605 (21)	O23	1.573 (20)
mean	1.609		1.606		1.595
Si2-O2	1.635 (23)	Si6-O7	1.600 (20)	Si10-O16	1.510 (21)
O5	1.576 (11)	O17	1.536 (24)	O21	1.606 (17)
O6	1.632 (20)	O18	1.550 (25)	O23	1.689 (21)
O7	1.609 (22)	O19	1.643 (26)	O24	1.535 (21)
mean	1.613		1.582		1.585
Si3-O3	1.567 (28)	Si7-O8	1.622 (18)	Si11-O10	1.605 (22)
O8	1.624 (25)	O11	1.528 (28)	O20	1.600 (21)
O9	1.616 (21)	O14	1.626 (21)	O24	1.619 (21)
O10	1.622 (23)	O20	1.592 (22)	O25	1.561 (23)
mean	1.607		1.592		1.596
Si4-O4	1.535 (31)	Si8-O9	1.516 (25)	Si12-O13	1.588 (22)
O11	1.651 (28)	O15	1.631 (21)	O19	1.550 (26)
O12	1.545 (24)	O17	1.624 (24)	O25	1.615 (25)
O13	1.563 (19)	O21	1.594 (17)	O26	1.633 (12)
mean	1.573		1.591		1.597

N-C1	1.86 (13)	F-C1	2.88 (13)	C1-C2	1.76 (16)	C7-C8	1.29 (10)
C4	1.85 (14)	C7	2.11 (9)	C2-C3	1.56 (16)	C8-C9	1.56 (9)
C7	1.53 (8)	C8	2.20 (7)	C4-C5	0.79 (18)	C3-C6[b]	3.09 (14)
F	2.45 (10)			C5-C6	1.31 (16)	C9-C9[b]	2.72 (12)

Si1-O1-Si1	134.9 (1.2)	Si3-O10-Si11	158.7 (1.5)	Si6-O19-Si12	152.3 (1.7)
Si1-O2-Si2	147.9 (1.1)	Si4-O11-Si7	164.5 (1.3)	Si7-O20-Si11	156.9 (1.8)
Si1-O3-Si3	144.9 (1.6)	Si4-O12-Si9	153.1 (1.6)	Si8-O21-Si10	148.7 (1.3)
Si1-O4-Si4	163.7 (2.0)	Si4-O13-Si12	153.2 (1.6)	Si9-O22-Si9	150.3 (1.6)
Si2-O5-Si2	144.0 (1.5)	Si5-O14-Si7	143.0 (1.4)	Si9-O23-Si10	142.7 (1.3)
Si2-O6-Si5	143.2 (1.2)	Si5-O15-Si8	148.6 (1.7)	Si10-O24-Si11	178.6 (1.3)
Si2-O7-Si6	151.9 (1.8)	Si5-O16-Si10	171.3 (1.4)	Si11-O25-Si12	145.0 (1.6)
Si3-O8-Si7	143.8 (1.6)	Si6-O17-Si8	178.1 (1.3)	Si12-O26-Si12	148.7 (1.4)
Si3-O9-Si8	156.2 (1.9)	Si6-O18-Si9	173.9 (1.8)		

[a] Standard deviation (1σ) in parentheses. [b] Distances between end atoms of adjacent complexes.

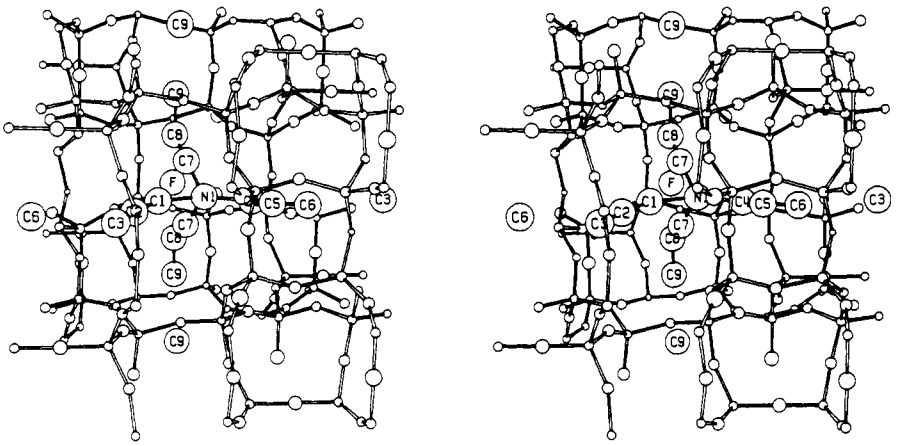

Figure 6. Stereoview of the refined positions of one TPAF complex and its relation to the surrounding portion of the silica framework and end C atoms of adjacent complexes. The N atom lies near the origin of the four arrows at the upper left of Figure 5, and the C8 and C9 atoms lie nearly in the center of a straight channel parallel to *b*. The C1–C6 atoms lie in a mirror plane, and the C1–C3 and C4–C6 limbs point along adjacent zig and zag portions of a zig-zag channel. The nonplanar rings of ten Si atoms and ten O atoms that limit each type of channel are shown, and detailed dimensions are given in Figure 7.

to convert each propyl into a butyl limb. Similarly, the end C9 atoms of two propyl limbs pointing along a straight channel also approach too closely to allow replacement of propyl by butyl. Seven of the C atoms, plus the F atom, lie within 3.6–3.9 Å of the oxygen atoms (Table III), and the propyl limbs lie neatly in positions consistent with van der Waals bonding. It is important to emphasize that the dimensions of the channels may change as the TPAF complex is removed. Hence the applicability of the dimensions of the limiting 10-rings (Figure 7) to *detailed* discussion of the molecular sieve properties after calcination is somewhat restricted. In the precursor, the free area of the straight channel is near elliptical, with major and minor axes of 5.8 and 5.2 Å. This assumes that the effective radius of the oxygen atom is 1.35 Å and that the nonplanarity of the 10-ring is unimportant. The free area of the zig-zag channel is even more nonplanar, and the maximum and minimum free distances of 5.6 and 5.3 Å should probably be modified to a near-circular effective cross section with diameter ~5.3 Å. The above dimensions differ slightly from the apertures of 5.6 × 5.4 Å for the straight channel and 5.5 × 5.1 Å for the sinusoidal channel reported in ZSM-5.[15] The channel dimensions are consistent with sorption of molecules as large as benzene (kinetic diameter 5.85 Å) and rejection of molecules larger than 6 Å such as neopentane (kinetic diameter 6.2 Å). Details now follow.

Framework Topology and Subunits. Identification of subunits is important because new frameworks have been invented by finding different linkages and because subunits may be involved in synthesis.

The most obvious structural unit in the silicalite and the ZSM-5 frameworks (stereoplots in ref 5 and 15) is a two-dimensional

Table III. Framework to Complex Distances (Å) Less Than 4.2 Å

C1-O5	3.68 (0.10)	C7-O23	4.09 (0.08)
O6	3.85 (0.08)	O8	4.15 (0.08)
C2-O6	3.81 (0.10)	C8-O7	3.84 (0.08)
O5	3.83 (0.12)	O13	3.91 (0.08)
O14	3.93 (0.04)	O12	3.91 (0.08)
C3-O25	3.56 (0.08)	O6	3.93 (0.07)
O26	3.65 (0.11)	O19	3.98 (0.08)
O20	3.82 (0.03)	O23	3.99 (0.08)
C4-O1	3.73 (0.11)	O14	4.10 (0.08)
O21	4.02 (0.04)	C9-O14	3.85 (0.07)
O23	4.05 (0.09)	O8	4.08 (0.07)
O3	4.11 (0.09)	O23	4.12 (0.06)
O9	4.11 (0.05)	O13	4.12 (0.07)
C5-O1	3.63 (0.15)	O21	4.15 (0.05)
O21	3.95 (0.05)	O7	4.17 (0.06)
O9	4.14 (0.06)	O6	4.18 (0.06)
O23	4.15 (0.13)	O12	4.20 (0.07)
O3	4.18 (0.12)	F-O13	3.75 (0.06)
O15	4.18 (0.07)	O19	3.83 (0.06)
C6-O5	3.62 (0.15)	O12	3.85 (0.06)
O15	3.81 (0.04)	O7	4.17 (0.06)
O6	3.95 (0.11)		
O1	4.09 (0.14)		
O21	4.10 (0.06)		

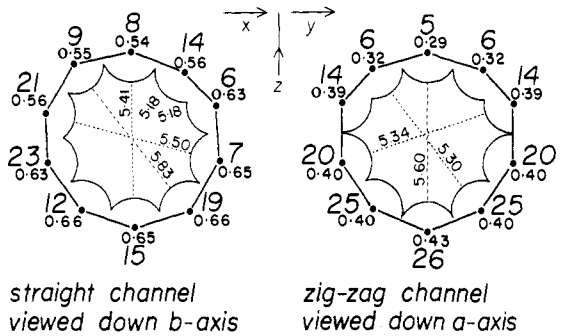

Figure 7. Dimensions of limiting 10-rings of oxygens in the straight and zig-zag channels. Each large number specifies the type of oxygen, and the small number gives either the z coordinate (left) or the x coordinate (right). Each oxygen has a formal radius of 1.35 Å. Note the elliptical and near-circular projections of the limiting areas.

sheet[3] of 5-, 6-, and 10-rings that occurs in both the a- and b-axis projections. This sheet is also found in a c-axis projection of the framework of the zeolite ferrierite and in the a-axis projection of the proposed framework[20] of ZSM-11. A formal description of this sheet is $(5^26)_1(5^210)_1(5.6.10)_1$, which expresses the occurrence of three types of three-connected nodes of equal population (subscript 1) but lying at the intersection of different circuits (e.g., two 5-rings and one 6-ring meeting at the first node). From each three-connected node, a fourth branch goes either upward or downward with associated buckling of the sheet to generate a three-dimensional four-connected framework, whose circuit symbol[21] is $(4.5^3.6.7)_2(5^58)_4(5^46^2)_3(5^46.8)_1(5^36^27)_1(5^26^37)_1$. The high fraction of 5-rings (~two-thirds) is a feature shared with the zeolites bikitaite, dachiardite, mordenite, ferrierite, and epistilbite. Five-rings also occur in the coesite, keatite, and melanophlogite polymorphs of silica. Because melanophlogite has a fairly open framework[22] that can enclose organic matter and coesite[23] has a dense framework, the presence of 5-rings is not simply related to the porosity of a framework.

Because of the occurrence of a two-dimensional hexagonal sheet of linked tetrahedral nodes (6^3) in dachiardite, mordenite, ferrierite, and epistilbite,[24,25] it is interesting to note that triple bands

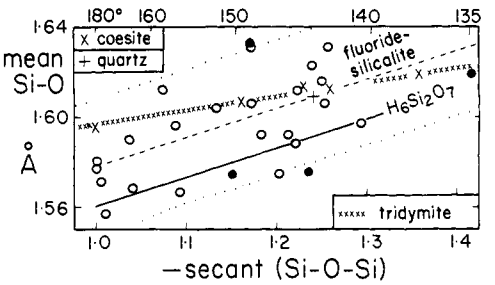

Figure 8. Relationship between the mean distance from two Si atoms to an oxygen and the secant of the Si-O-Si angle for the fluoride silicalite precursor ($4TPAF{\cdot}96SiO_2$) and three other polymorphs of SiO_2. Individual values are shown for quartz[29] and coesite,[30] while only the trend is shown for tridymite.[31] The filled and open circles for the fluoride silicalite precursor are respectively for O atoms on and off the mirror planes in *Pnma*. The trend for $H_6Si_2O_7$ was calculated.[28]

of corrugated 6-rings lie parallel to the a axis of silicalite. Four rings and dimers are needed to cross-link the triple bands, as illustrated by a model built from colored tetrahedral stars shown on the cover page of issue 5645 of *Nature*.[3] This cross-linking produces a corrugation of each triple band, and the displacement of the tetrahedral nodes along the a axis is up–down–up–up–down–up–down–down. The simplest sequence up–down yields a family of polytypic nets whose channel system, to be described elsewhere, contains straight channels limited by 10-rings that are interconnected by straight channels limited by 8-rings. The transformation of the silicalite or the ZSM-5 net to the ZSM-11 net[6] destroys the triple band of hexagons, and only a triplet of hexagons survives. Neither the sheet nor the triple band is suitable as a "secondary building unit".[26]

Geometry and Estimated Charge of Silica Framework. Although interpretation of the geometrical properties of silicate frameworks is difficult because of the interaction with other cations and molecules and because of substitution of Si by Al, etc., molecular-orbital concepts have proven useful for zeolites.[27] Even for silica frameworks, there is great difficulty in understanding the geometrical features because of inability to obtain an exact solution of the wave equation. In principle, silicalite would be an important test of chemical models if accurate measurements could be made of the atomic coordinates, but various technical problems (twinning, pseudosymmetry, small crystal size) have ruled out measurements of sufficient accuracy in existing experiments.

In the meantime, the data for the fluoride silicalite precursor (Figure 8) are generally consistent with predictions for the decrease of the mean of the two Si–O distances to an oxygen atom as the Si–O–Si angle increases up to 180°. The solid line is based on ab initio STO-SG molecular orbital calculations for an $H_6Si_2O_7$ cluster,[28] and the data for the fluoride silicalite precursor fit within an error band of ±0.03 Å about a parallel dashed line. However, the observed data for three polymorphs of silica (quartz,[29] coesite,[30] and tridymite[31]) fall neatly about a line of lesser slope that crosses the dashed line for the fluoride silicalite precursor. It will be necessary to increase the accuracy of data for silicalite materials by at least a factor of 4 before further progress can be made.

Because the values of the Si–O–Si angles are accurate to <2° (1σ), they can be used for speculation on the theoretical charge density of oxygen atoms. In particular, molecular-orbital calculations[32] for T_5O_{13} clusters predicted that the electrical charge varies from −1.22 for an Si–O–Si angle of 180° to −1.28 for an angle of 134°. Hence oxygens 16, 17, 18, and 24 should have

(20) Kokotailo, G. T.; Chu, P.; Lawton, S. L.; Meier, W. M. *Nature (London)* **1978**, *275*, 119–120.
(21) Smith, J. V. *Am. Mineral.* **1978**, *63*, 960–969.
(22) Kamb, B. *Science (Washington, D.C.)* **1965**, *148*, 232–234.
(23) Araki, T.; Zoltai, T. *Z. Kristallogr.* **1969**, *129*, 381–387.
(24) Meier, W. M. "Natural Zeolites"; Pergamon: Oxford, England, 1978; pp 99–104.
(25) Merlino, S. *Rend. Soc. Ital. Mineral. Petrol.* **1975**, *31*, 513–540.
(26) Meier, W. M. *SCI Monogr.* **1968**, 10–27.
(27) Gibbs, G. V.; Meagher, E. P.; Smith, J. V.; Pluth, J. J. *ACS Symp. Ser.* **1977**, *40*, 19–29.
(28) Newton, M. D.; Gibbs, G. V. *Phys. Chem. Miner.* **1980**, *6*, 221–246.
(29) Le Page, Y.; Donnay, G. *Acta Crystallogr., Sect. B* **1976**, *B32*, 2456–2459.
(30) Gibbs, G. V.; Prewitt, C. T.; Baldwin, K. J. *Z. Kristallogr.* **1977**, *145*, 108–123.
(31) Konnert, J. H.; Appleman, D. E. *Acta Crystallogr., Sect. B* **1978**, *B34*, 391–403.
(32) Hill, R. J.; Gibbs, G. V. *Acta Crystallogr., Sect. B* **1979**, *B35*, 25–30.

the smallest charges, and oxygen 1 the largest charge.

Position of the TPAF Complex. Although the atomic coordinates in Table I are an average of spatially disordered sites and although some systematic error results from refinement in a space group of pseudosymmetry, the positions of the propyl limbs and the central N atoms are sufficiently accurate to permit discussion of interaction between adjacent complexes. The distances between the end C atoms (C3–C6, 3.09 ± 0.14; C9–C9 2.72 ± 0.12 Å) are consistent with van der Waals interactions, and there is insufficient room for replacement of propyl by butyl. Because seven of the C atoms lie less than 4 Å from at least one framework oxygen of the channel walls, it does not seem reasonable to replace a propyl limb by a strongly buckled butyl limb. It would be possible to replace TPA by equal amounts of TEA (E, ethyl) and TBA (B, *n*-butyl) if the TEA and TBA alternated so that each TEA was in contact with four TBA, and vice versa. Other combinations of paired complexes would be geometrically feasible, or indeed a large complex might occupy only alternate sites while the intervening ones stayed vacant.

The actual position of the TPAF complex must be determined by a complex balance between various forces. Because the zig–zag and straight channels do not meet (Figure 5) at the angle of a regular tetrahedron (109.5°), the tetrahedrally bonded N atom cannot lie at the geometric center of the intersection of the channels, and indeed the actual coordinates ($x = 0.450$, $y = {}^3/_4$, and $z = 0.105$) are considerably displaced from the calculated center at $x = 0.5$, $y = {}^3/_4$, and $z = 0.0$. To compensate for the four angles of 90° and one angle of 112.5° between the arrows of Figure 5, the N atom moves away from the center of the straight channel but is constrained onto the mirror plane (Figure 6). The C–C bonds "swivel" into convenient positions.

A second factor results from van der Waals bonding. There must be strong van der Waals interaction between end atoms C9 at 2.72 Å and a weaker interaction for atoms C3 and C6 at 3.09 Å (assuming that these distances are significantly different). It appears that each propyl limb moves away from the center of a channel where it would be rather far away from framework oxygens (just over 4 Å) for van der Waals bonding so that some of the C atoms can approach at least one framework oxygen at distance of ~3.6–3.8 Å. Although the low accuracy of the measured distances in Table III provides poor justification for this suggestion, it appears plausible for C1–C6 in the two propyl limbs bent away from the F atom.

A third factor is the tendency of the F atom to be (a) enwrapped by C7 and C8 atoms at 2.1 Å from propyl limbs projecting up the straight channel, by N at 2.4 Å, and to a lesser degree by C1 at 2.8 Å and (b) positioned within van der Waals bonding distance (~3.8 Å) to six framework oxygens of types O12, O13, and O19. Such a configuration of the fluorine atom (or fluoride anion for an ionic model) is physically reasonable and similar to the configuration described in the TPABr structure.[33] Probably the fluoride ion is held in place by electrostatic interactions involving hydrogen bonding to the methylene groups in the TPA complex. Previously reported[34] bond lengths for hydrogen bonds involving F^- (2.3–2.8 Å) encompass the present values when experimental errors are considered. It must be emphasized again that positional disorder of the TPAF complex, especially for the F position (Figure 4), makes it unwise to overinterpret the details of the bond distances and angles. This also applies to the C–C distances whose individual values of 0.79–1.76 Å scatter about the mean of 1.38 Å because of poor resolution of the electron density peaks (Figure 3).

Because each propyl limb is "narrower" than the surrounding channel for van der Waals distances of 4 Å, each TPAF complex can be spatially disordered, and such disorder may be responsible for the optically monoclinic symmetry. A structure determination at low symmetry should provide a test.

Possibility of Template Control of Crystallization. The neat fit between the TPAF complex and the silica framework that clathrates it further supports a template mechanism like that proposed for silicalite,[3] in which the silica tetrahedra assemble around the complex during crystallization. It appears likely that a tetrapropylammonium (TPA) complex is the preferred alkylammonium template for the crystallization of fluoride silicalite and other materials with the same framework topology, e.g., silicalite[3,11] and ZSM-5,[4,15] because its specific size and shape best fit the channel system with one complex occupying each intersection.

The calculation that butyl limbs cannot reasonably replace propyl limbs one for one in this structure is consistent with the observed preferred crystallization from TBA and TBP (tetra-*n*-butylphosphonium) systems of a closely related but different framework topology, that reported for ZSM-11.[20] Although the volumes of the channel systems in the ZSM-11 and silicalite-type framework are similar, the four-channel intersections for each 96 TO_2, equivalent in silicalite, occur instead as large and small pairs in ZSM-11. Since (a) sufficiently accurate ZSM-11 framework atom positions are not known and (b) analyses suggest only partial occupation of the intersections by the tetra-*n*-butyl complex (0.6 TBP per intersection[35]), detailed speculation on placement of the organic complex is not warranted.

One intriguing observation possibly bearing information on the nature of the nucleus is the development of growth twinning in many specimens of silicalite[3] and fluoride silicalite precursors. For the fluoride silicalite precursor, the twin law of 90° rotation about the *c* axis together with the twin morphology implies that the original growth nucleus may have begun with tetragonal symmetry followed by a switch to orthorhombic in which one twin unit of the precursor inherited the tetragonal *a* and *b* axes for its orthorhombic *a* and *b* axes, whereas the other twin unit inherited tetragonal *b* and *a* for its orthorhombic *a* and *b*. If twinning developed on both (100) and ($\bar{1}00$) to give one twin orientation, and on both (010) and ($0\bar{1}0$) to give the second, and if all twin sectors grew at approximately the same rate, the twin intergrowth in Figure 2 might be explained. Lattice imaging by electron microscopy through a central section of a silicalite twin should allow a test.

Despite the observed neat fit and positive role of TPA in nucleating and crystallizing materials with this framework topology, extreme caution is needed in proposing a specific template role for TPA. Any such proposal must consider the ability to nucleate and crystallize a zeolite with apparently the same topology, LZ-105,[36] in the absence of any organic template or seed material.

Acknowledgment. The National Science Foundation is thanked for Grant CHE 80-23444 and for general support to the Materials Research Laboratory. Technical support at Chicago from T. Araki, I. M. Steele, and I. Baltuska is acknowledged, as is assistance and advice at Tarrytown from E. M. Flanigen. A helpful review by R. M. Hazen is appreciated.

Registry No. Silica tetrapropylammonium fluoride, 82891-68-7.

Supplementary Material Available: Table IV, a list of observed and calculated structure factors (10 pages). Ordering information is given on any current masthead page.

(33) Zalkin, A. *Acta Crystallogr.* **1957**, *10*, 557–560.
(34) Durrant, P. J.; Durrant, B. "Advanced Inorganic Chemistry"; Wiley: New York, 1964.
(35) Chu, P. U.S. Patent NM3 709 979, 1973.
(36) Grose, R. W.; Flanigen, E. M. U.S. Patent NM4 257 885, 1981.